

SYNTHESIS, CHARACTERIZATION, AND PHOTOCATALYTIC BEHAVIOUR OF NANOCRYSTALLINE ZnO, TiO₂ AND ZnO/TiO₂ NANOCOMPOSITES

V. RAJENDAR^{a,c}, Y. RAGHU^b, B. RAJITHA^c, C.S. CHAKRA^b, K.V. RAO^d, S. H. PARK^{a*}

^a*Department of Electronic Engineering, Yeungnam University, Gyeongsan-si, Gyeongsangbuk-do, 38541, Republic of Korea*

^b*Center for Nanoscience and Technology, Institute of Science and Technology, Jawaharlal Nehru Technological University Hyderabad, Telangana State, 500085, India*

^c*Department of Physics, BVRIT Hyderabad College of Engineering for Women, JNTUH, Hyderabad, Telangana State, 500085, India*

^d*School of Medicine, Radiology department, Johns Hopkins University, Baltimore, USA*

^e*Department of Physics, B.V. Raju Institute of Technology, Narsapur, Medak, Telangana State, 502313, India*

ZnO and TiO₂ nanoparticles (NPs) and ZnO/TiO₂ nanocomposites (NCs) were prepared by a solution combustion synthesis method. The samples were characterized by X-ray diffraction (XRD), field emission scanning electron microscopy (FESEM), transmission electron microscopy (TEM), and ultraviolet– visible spectroscopy. The photocatalytic activity of the ZnO/TiO₂ NC under sunlight for the degradation of methylene blue (MB) and crystal violet (CV) was compared with that of the individual ZnO and TiO₂NPs. The effects of the sample concentration and contact time on the degradation efficiency of both dyes were investigated. The contact time was found to have greater impact on the degradation of the dyes than the sample concentration used for degradation. The ZnO/TiO₂NC had 5% greater dye removal efficiency than the individual ZnO or TiO₂NPs.

(Received April 7, 2017; Accepted May 20, 2017)

Keywords: Nanoparticles; Nanocomposites; Photocatalytic activity; Efficiency

1. Introduction

Over the past few decades, the discharge of toxic effluents into water reservoirs, such as lakes and rivers, remains an important ecological concern. In particular, textile dyes have a great impact on flora and fauna at scales that can adversely affect the biosphere. For example, textile dyes reduce light penetration and prevent the photosynthesis of submerged plants [1-3]. Furthermore, they can react with other effluents in the water, resulting in stable toxic chemicals that reach humans through the soil. Therefore, there is an urgent need for effective treatment processes for the purification of these dyes [4]. Nanoparticles and nanotechnology-based solutions have gained popularity in the water purification industry owing to their large surface area and higher catalytic potential compared to their bulk counterparts.

Over the past decade, the use of NPs, such as gold [5], silver [6], copper sulfide [7], zinc oxide [8], titanium dioxide [9], lead oxide [10], zirconium oxide [11] and montmorillonite [12] for the catalytic degradation of textile dyes and toxic effluents have been reported. Of these, NPs with photocatalytic degradation capabilities have attracted significant interest because of the use of natural light sources as the trigger for the breakdown of toxic effluents [13]. Recently, the use of NCs, as opposed to single phase NPs, have shown further improvement in the photocatalytic

*Corresponding author: sihyun_park@ynu.ac.kr

degradation of textile dyes, such as methylene blue and methyl orange [14]. The increased activity has sparked research into a range of multiphase nanomaterials. ZnO and TiO₂ are well known for their photocatalytic properties with a closely related direct bandgap of 3.3 and 3.2 eV, respectively [15]. ZnO&TiO₂ are less expensive, nontoxic, and most successful semiconductor photocatalysts. These photocatalysts are applicable to a wide range of organic synthetic dyes [16].

Some researchers have synthesized ZnO, TiO₂ and their composites for photocatalysis application through various methods, including sol-gel, hydrothermal, wet chemical method, green synthesis, co-precipitation and combustion techniques. The combustion process had significant advantages compared to other methods such as low processing temperature, simplicity, low-cost, low hazardousness and ease of handling. Moreover, it can possibly be used to grow the nanostructures [17]. Therefore combustion method has been used to prepare of ZnO/TiO₂NC [18].

Now research trends on phototocatalytic activity of dye degradation efficiency. Recently, Sharam Moradi *et al.* [19] reported the effect of photocatalytic behaviour of ZnO NPs and Christos A *et al.* [20] reported the photocatalytic activity of TiO₂ by the degradation efficiency of MB only. Few studies have also reported with ZnO/TiO₂ NC photocatalytic activity with MB [21]. In this case, the photo induced charge carrier in single bare semiconductor particles has a very short life time because of the high recombination rate of the photo generated electron/holepairs, which reduces photocatalytic efficiency and hinders further use of particles. Therefore, improving photocatalytic activity by modification has become an important task among researchers in recent years. On the other hand, very little research has been conducted on the combined photocatalytic effects of these NCs on the degradation of textile dyes, such as MB or CV.

This manuscript reports the photocatalytic activity of ZnO/TiO₂NC for both MB and CV. Here we are going to discuss ZnO/TiO₂ NC with MB and CV because of having more strength of removing effluents from water. The main aim of the present work is to discuss the synergistic potential of a 1:1 ZnO and TiO₂NC for the degradation of MB and CV under ambient sunlit conditions. The effects of the contact time and NC concentration on the degradation of the dyes are also discussed in detail. Furthermore, a comparison of the efficiency of the individual nanoparticle components against the NCs was also performed.

2. Experimental procedures

Zinc nitrate hexahydrate (MERCK Chemicals Ltd, UK), ascorbic acid (FINAR Chemicals Ltd, India), titanium isopropoxide (Avra Chemicals Ltd, India), and glycine (FINAR Chemicals Ltd, India) were used as the precursors for the preparation of NCs. Distilled water was used as the solvent in all the experiments. All the chemicals were used in their original state and were not subjected to additional purification steps.

2.1. Preparation of zinc oxide and titanium dioxide nanoparticles

Zinc oxide and titanium dioxide NPs were prepared by a combustion synthesis process. In a typical synthesis step to prepare zinc oxide NPs, zinc nitrate hexahydrate and ascorbic acid were dissolved in distilled water at 1:0.3 molar ratios and heated on a hot plate at 300°C until a brown precipitate formed. The precipitate was crushed finely and calcined at 400°C. The resulting powder was white and consisted of ZnO NPs. TiO₂ NPs were prepared using a similar process using titanium isopropoxide and glycine as the precursors. The structural, morphological and optical properties of the prepared NPs were characterized before being used for preparation of the NCs.

2.2. Preparation of the ZnO/TiO₂ nanocomposites

The ZnO and TiO₂NPs prepared in the previous step were mixed at a 1:1 weight ratio in a measuring cylinder using distilled water. A well dispersed solution was prepared by vigorous stirring of the NPs followed by ultrasonication for 1 h. The dispersion was then heated at 100°C to obtain a dry powder that was labeled the ZnO/TiO₂NC. All the samples were characterized by scanning electron microscopy, transmission electron microscopy, particle size analysis, X-ray

diffraction and UV-Visible spectrometry.

2.3. Adsorption and photocatalytic degradation

Adsorption and photocatalytic degradation experiments were carried out on 50 ppm (1 mg/mL) stock solutions of MB and CV. The role of the adsorption time was determined by incubating various concentrations (2, 4, 6, 8, and 10 mg/mL) of ZnO and TiO₂NPs with the MB and CV stock solutions in the dark for 75 min. The same experiments were conducted on the ZnO/TiO₂NCs. The adsorption time/contact time efficiency was determined by UV-visible spectroscopy at the end of the speculated time. The role of the NC concentration on the photocatalytic degradation efficiency was determined by exposing various concentrations (2, 4, 6, 8, 10 mg/mL) of ZnO and TiO₂NPs to sunlight for different times (15, 30, 45, 60, and 75 min). The same set of experiments was conducted on the ZnO/TiO₂NCs. All the experiments were conducted in 15 mL test tubes using 10 mL of the batch solutions at noon in broad daylight with no cloud cover. All the experiments were performed in triplicate with errors below 5%; the average values are reported. The decolorization/removal efficiency was calculated using the following equation:

$$\% \text{removal efficiency} = (C_0 - C_1)/C_0 \times 100$$

where C_0 is the initial concentration and C_1 is the instantaneous concentration of the sample. The kinetics of dye degradation could be described by pseudo first order kinetics.

3. Results and discussion

3.1. XRD analysis

Structural analysis of both samples was conducted using an X-ray Diffraction system. As expected, the samples showed a single phase nature with reflections matching JCPDS #89-0510 for ZnO and JCPDS#21-1272 for TiO₂. The XRD patterns for the composite system revealed the presence of reflections from both ZnO and TiO₂ in equal strength representing the equal crystalline distribution of phases within the sample. Fig. 1(a), 1(b) and 1(c) present XRD patterns of the ZnO, TiO₂ and ZnO/TiO₂NC samples, respectively. The average crystallite sizes of the samples, which were calculated using the Debye Scherer formula, were 24.9, 25.3 and 19.5 nm for ZnO, TiO₂ and ZnO/TiO₂ NC respectively.

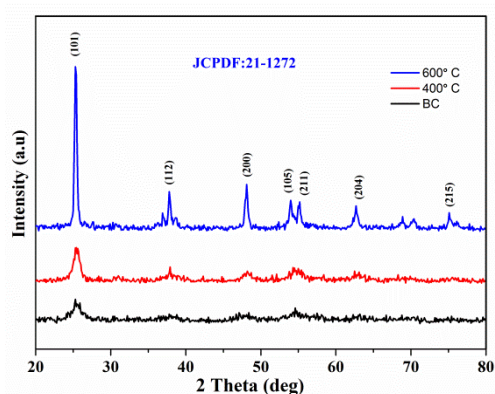


Fig. 1(a): XRD pattern of typical samples obtained before calcination (BC) and at different annealing temperatures and JCPDS cards of ZnO

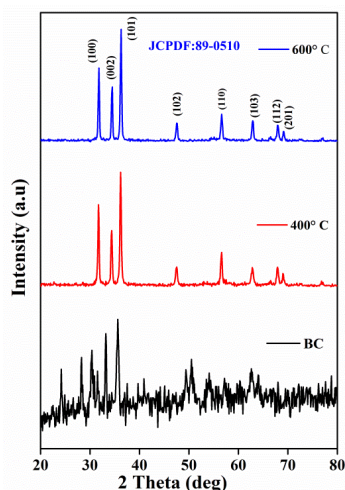


Fig. 1(b): XRD pattern of typical samples obtained before calcination (BC) and at different annealing temperatures and JCPDS cards of TiO₂

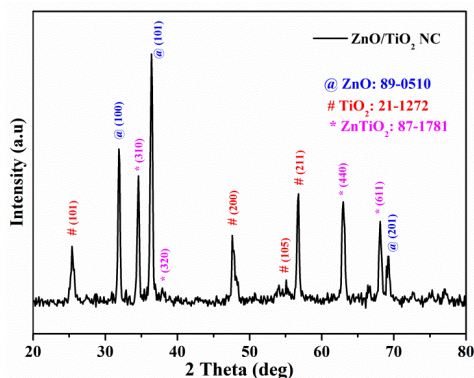


Fig. 1(c): XRD pattern of typical samples and JCPDS cards of ZnO, TiO₂ and ZnTiO₂

3.2. Particle size analysis

Particle size analysis was conducted using 5 mL of 1 mg/mL ethanolic suspensions of the ZnO and TiO₂NPs. The suspensions were sonicated for 10 min before taking the readings. Fig. 2(a) and 2(b) present the particle size distribution histograms for the ZnO and TiO₂ samples, respectively. The size of the NPs ranged from 10 to 100 nm. The mean particle size of the ZnO and TiO₂NPs, as calculated from the histograms, were 32.3 nm and 34.5 nm, respectively. Particle size analysis of the ZnO/TiO₂NC had a mean particle size of 29.7 nm with a similar size distribution, as shown in Fig. 2(c).

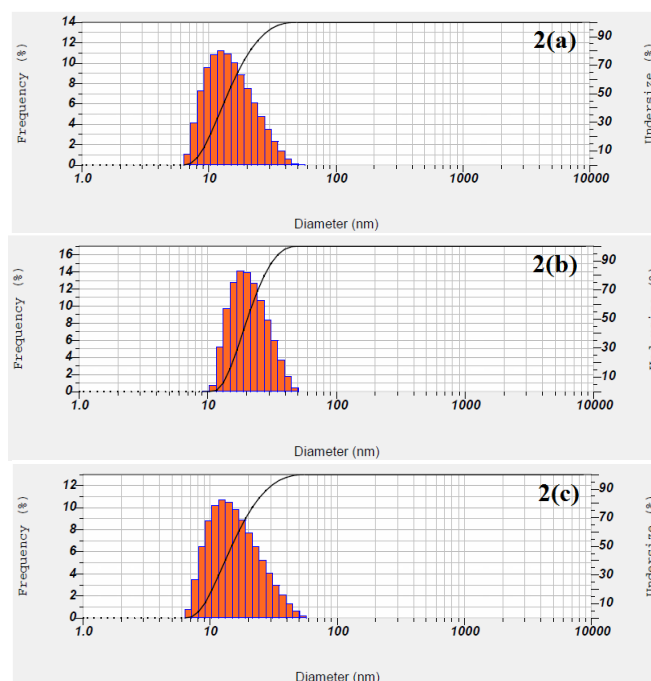


Fig. 2(a-c): Particle distribution of ZnO NPs (2a), TiO₂NPs (2b) and ZnO/TiO₂NCs (2c)

3.3. Morphology of the nanoparticles

The morphology of the NPs was determined by examining the samples by SEM and TEM. Fig. 3(a) and 3(d) show the homogenous distribution of multifaceted ZnO NPs in the size range, 25-30 nm. These results are concurrent with the particle size analysis and the crystallite size analysis discussed in the previous section. Energy dispersive X-ray spectroscopy (EDS) indicates that the samples contained only Zn and O, revealing the purity of the sample. Fig. 3(b) and 3(e) show the large agglomerated structures comprised of smaller spherical NPs in the size range, 20-30 nm. EDS indicated the presence of Ti and O in the sample, revealing the purity of the prepared product. The particle sizes measured from these images strongly agree with the crystallite size and particle size analysis discussed in the previous sections. Furthermore, Fig. 3(c) and 3(f) show the heterogeneous distribution of ZnO and TiO₂NPs in the NC sample. The NPs were distributed equally over the surface indicating the presence of the samples at a 1:1 ratio. In addition, EDS revealed an equal atomic distribution of the Zn and Ti across the sample.

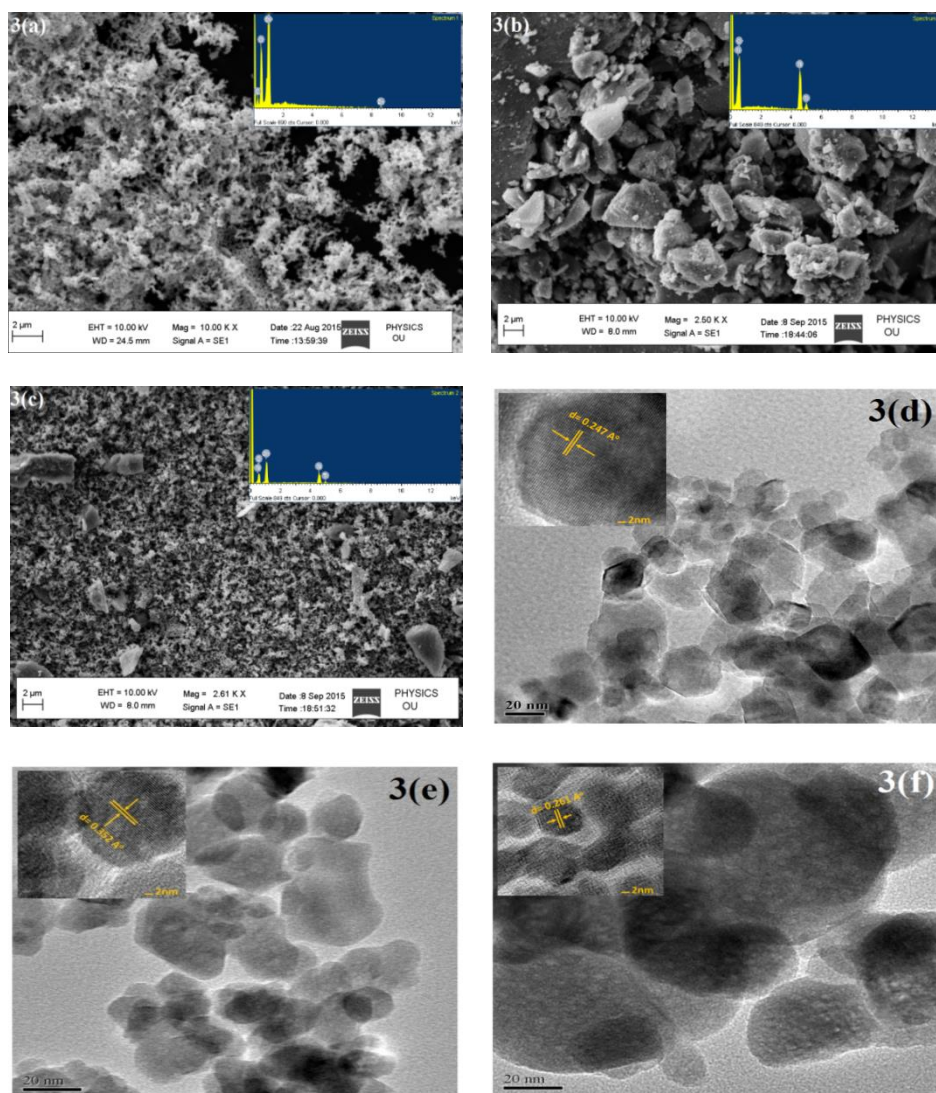


Fig. 3. SEM images of the ZnONPs(a), TiO₂NPs (b) and ZnO/TiO₂NCs (c)
TEM images of the ZnONPs(d), TiO₂NPs (e) and ZnO/TiO₂NCs (f)

3.4. UV-Visible spectroscopy

A 5mL sample of 1mg/mL aqueous suspensions of both ZnO and TiO₂NPs were used for UV-visible spectroscopy analysis. Fig. 4 show the results obtained for the ZnO and TiO₂ samples, respectively. The absorption peak for the ZnO sample was observed at 381.3 nm compared to 358 nm, which is the typical absorption maxima for bulk ZnO. The sharp peak indicates the presence of monodispersed NPs in the aqueous suspension. A band gap of 3.247 eV was calculated for the ZnO NPs compared to 3.46 eV for bulk ZnO.

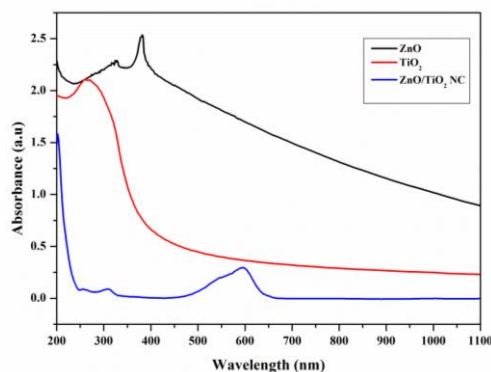


Fig. 4: UV/Vis spectrum of ZnO NPs, TiO₂NPs and ZnO/TiO₂NCs

UV-visible spectroscopy of the TiO₂ sample revealed the presence of an absorption peak at 261.8 nm with a calculated band gap of 4.73 eV. The large increase in the band gap from 3.2 eV (for bulk TiO₂) can be attributed to the lower particle size of the sample. The ZnO/TiO₂NC spectrograph (Fig. 4) revealed the presence of a supplementary peak at 581.6 nm in addition to those observed for the individual NPs. The supplementary peak may be attributed due to the synergetic response based on combinatorial effect of both ZnO and TiO₂NC in the presence of MB and CV. The presence of this additional peak in the visible region of the light spectrum suggests a synergetic response to sunlight for the NC compared to its individual counterparts.

3.5 Photocatalytic Degradation

3.5.1. Effect of adsorbent concentration

In this experimental set, the NPs and dyes were mixed and exposed to sunlight. The samples were collected at regular times to evaluate the extent of dye degradation. The results (Fig. 5(a-f)) showed that the efficiency of degradation was linear and increasing for all samples against both MB and CV. In addition, at lower concentrations, the ZnO NPs had lower degradation efficiency compared to the TiO₂NPs. On the other hand, the total dye removal efficiency was greater for the ZnO NPs than for the TiO₂NPs. Interestingly, the NC showed a slow initial response regarding the dye removal efficiency but revealed greater efficiency than both ZnO and TiO₂NPs at higher concentrations. Overall, even at different concentrations, the removal efficiency did not vary greatly, confirming that the reaction time is more important for dye removal than concentration of the material.

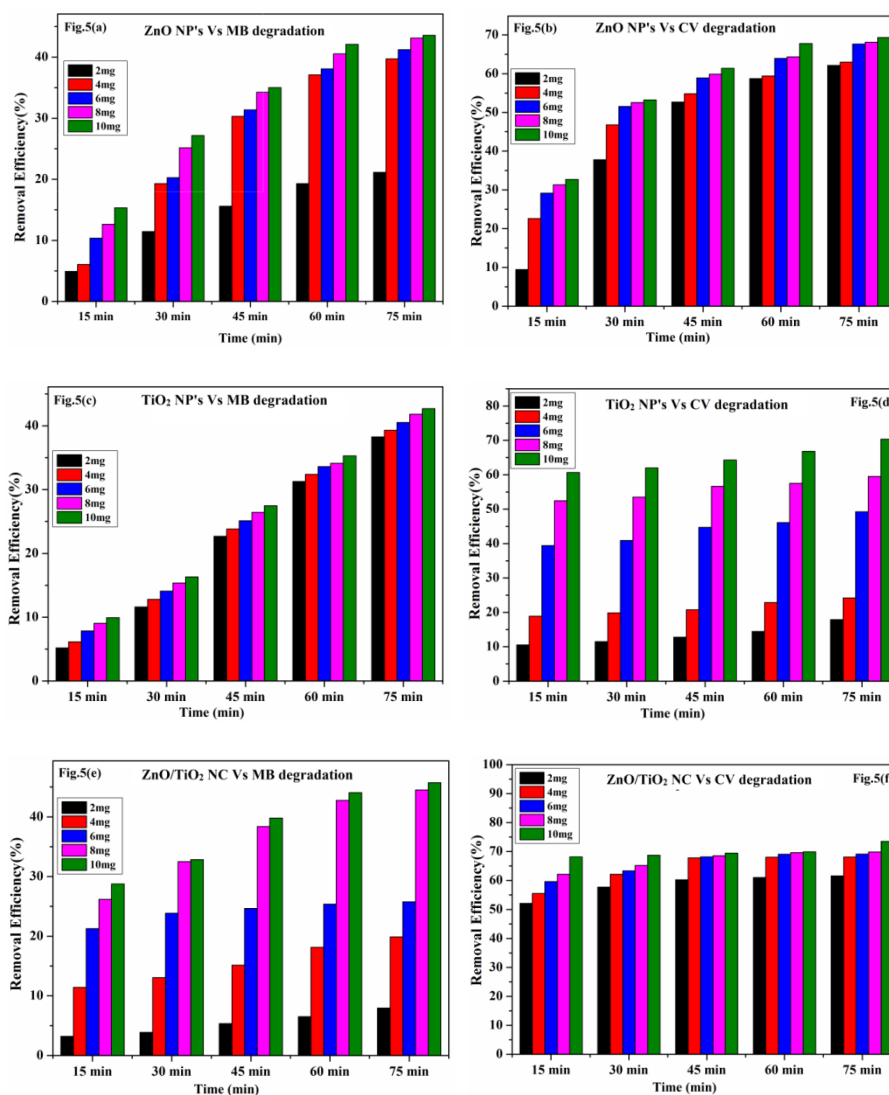


Fig. 5. Adsorbent dosage effect on MB and CV with respect to ZnO NPs (5a, 5b), TiO₂NPs (5c, 5d) and ZnO/TiO₂ NCs (5e, 5f)

3.5.2. Effect of Contact Time

As explained earlier, in this experimental set, different concentrations of NPs were incubated in the dark with both dyes for a period of 75 min before being exposed to sunlight. The dye removal efficiency was then determined for different reaction times after incubation. These results suggest that the initial incubation time increases the dye removal efficiency considerably at exposure times as low as 15 min. The dye removal efficiency of all the samples (Fig. 6(a-f)) in both dyes indicated the same pattern. The dye removal efficiency reached its maximum within the first 15 min of exposure, after which less than 5% change in efficiency was observed. These results were similar for all the samples and both dyes. The dye removal efficiency of the NC was greater in all four documented experiments. The ZnO/TiO₂ NC showed (Fig. 6 (e,f)) a 3% and 5% increase in removal efficiency for MB and CV, respectively, over the individual NPs at a 10 mg/L adsorbent concentration. Similarly, there was a respective 4% and 5% increase when the samples were pre-incubated in the dark. Interestingly, the degradation efficiency of all the NPs samples was greater on CV rather than on MB. This could be attributed to the greater chemical complexity of MB over CV. Table 1 lists all the data pertaining to the dye removal efficiency.

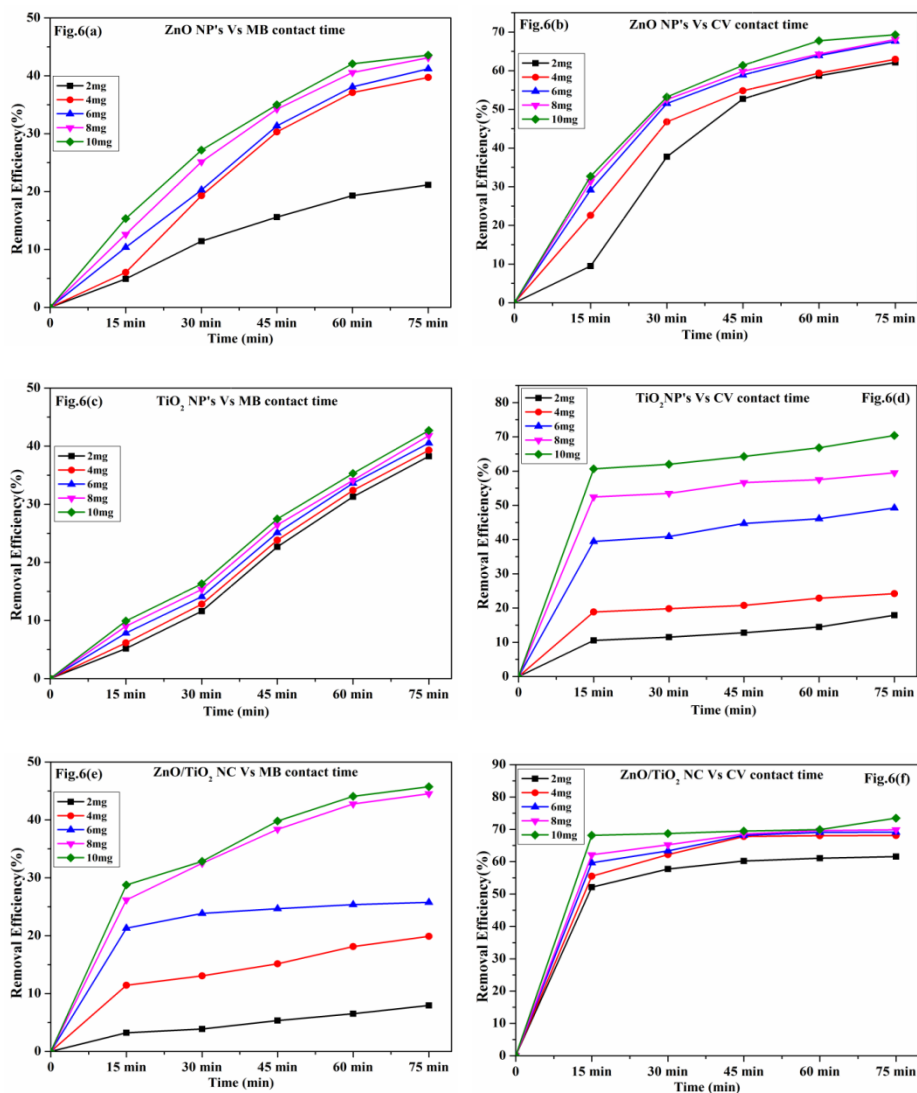


Fig. 6. Contact effect time on MB and CV with respect to ZnO NPs (6a, 6b), TiO₂ NPs (6c, 6d) and ZnO/TiO₂ NCs (6e, 6f)

Table 1: Effect of the adsorbent ZnO/TiO₂ NC dosage on MB and CV

Concentration of Sample (10mg/mL)	Dye Removal efficiency (%) in 50 ppm on MB				
	Time 15 min	Time 30 min	Time 45 min	Time 60 min	Time 75 min
ZnO NP's	15.34	27.17	35.01	42.09	43.58
TiO ₂ NP's	9.92	16.31	27.46	35.30	42.70
ZnO/TiO ₂ NC	28.76	32.83	39.79	44.06	45.73

Concentration of Sample (10mg/L)	Dye Removal efficiency (%) in 50 ppm on CV				
	Time 15 min	Time 30 min	Time 45 min	Time 60 min	Time 75 min
ZnO NP's	32.7	53.21	61.38	67.77	69.32
TiO ₂ NP's	60.66	61.98	64.27	66.82	70.37
ZnO/TiO ₂ NC	68.16	68.72	69.46	69.91	73.49

This clearly states that ZnO/TiO₂NC having more photocatalytic activity on MB & CV more efficiently than ZnO and TiO₂ alone. We assumed that the photo generated electrons moves

from the conduction band of excited ZnO to conduction band of TiO₂. In the same way photo generated hole also moves from valence band of ZnO to valence band of TiO₂. Such an efficient charge separation increases the life time of the charge carriers and increases the efficiency of the inter facial charge transfer to adsorbed substrates. MB & CV dyes are having the cationic nature, the photo generated electrons transfers to the surface of the adsorbed MB & CV molecules. The excited electrons presented in the photocatalyst conduction band moves into the molecular structure of MB & CV and disrupts its conjugated system which then leads to the complete decomposition of MB & CV molecules. Hole at the valence band generates OH[•] via reaction with water or OH⁻, might be used for oxidation of other organic compounds. Therefore, the efficiency of photo degradation of dye may arise due to reduction of electron-hole pair recombination in ZnO/TiO₂ NC and synergistic effect which depends on interaction among the metal oxide present in the ZnO/TiO₂NC [22].

4. Conclusions

ZnO and TiO₂ NPs prepared by the solution combustion synthesis method were mixed at a 1:1 ratio to prepare a ZnO/TiO₂ NC. The photocatalytic studies examining the effects of the sunlight exposure time and pre-exposure incubation time were conducted for the degradation of MB and CV. These results indicate a 5% higher dye removal efficiency for the NCs over the individual ZnO or TiO₂ NPs. The adsorbent concentration observations confirming that the reaction time will play an important role for dye removal than concentration of the material. The preliminary results presented in this work show much promise and suggest the need to further explore heterogeneous photocatalysis via visible light to address water contamination and environmental pollution.

Acknowledgment

The authors are grateful to the department of Electrical Engineering, Yeungnam University, Republic of Korea, Centre for Nano Science & Technology, Jawaharlal Nehru Technological University, Hyderabad, India and BV Raju Institute of Technology, Narasapur, Medak, India for providing the research facilities to undertake this work.

References

- [1] O. Pedersen, T.D. Colmer, K.S. Jensen. *Front Plant Sci.* **4**, 140 (2013)
- [2] H. Qian, L.A. Pretzer, C. Juan, Velazquez, Z. Zhao, M.S. Wong. *J. Chem. Technol. Biotechnol.* **88**, 735 (2013).
- [3] K. Roy, C.K. Sarkar, C.K. Ghosh. *Appl. Nanosci.* **5** (2015).
- [4] U. Shamraiz, A. Badshah, R.A. Hussain, M.A. Nadeem, S. Saba. Article in Press, *J. Saudi Chem. Soc.* DOI:10.1016/j.jscs.2015.07.005, (2015).
- [5] H. S. Hassan, M.F. Elkady, A.H. El-Shazly, H. S. Bamufleh. *J. Nanomater.* Article ID **967492** (2014).
- [6] M. Zeinab, A. Gamra, M.A. Ahmed. *Adv. in Chem. Eng. And Sci.* **5**, 373 (2015).
- [7] K. Meral, O. Metin. *Turk. J. Chem.* **38**, 775 (2014).
- [8] B. Pan, Q. Zhang, F. Meng, X. Li, X. Zhang, J. Zheng, W. Zhang, B. Pan. *J. Chen. Environ. Sci. Technol.* **47**, 6536 (2013).
- [9] L. Liu, B. Zhang, Y. Zhang, Y. He, L. Haung, S. Tan, X. Cai. *J. Chem. Eng. Data.* **60**, 1270 (2015).
- [10] M.T. Amin, A.A. Alazba, U. Manzoor. *Adv. Mater. Sci. Eng.* Article ID **825910** (2014).
- [11] P. Niu, J. Hao. *Colloids Surf. A Physicochem. Eng. Asp.* **431**, 127 (2013).
- [12] Md.A. Habib, Md.T. Shahadat, N.M. Bahadur, I.M.I. Ismail, A.J. Mahmood. *Int. Nano Lett.*

3, 1 (2013).

[13] S.A. Siuleiman, D.V. Raichev, A.S. Bojinova, D.T. Dimitrov, K.I. Papazova. *Bulg. Chem. Commun.* **45**, 649 (2013).

[14] S. Gunalan, R. Sivaraj, V. Rajendran. *Prog. Nat. Sci.* **22**, 693(2012).

[15] H.R. Ghaffarian, M. Saiedi, M.A. Sayyadnejad, A. M. Rashidi. *Iran. J. Chem. Eng.* **30**, (2011).

[16] M.M. Uddin, M.A. Hasnat, A.J.F. Samed, R.K. Majumdar. *Dyes and Pigments.* **75**, 207 (2007).

[18] V. Rajendar, T. Dayakar, K. Shobhan, I. Srikanth, K. Venkateswara Rao, *Superlattices and Microstructures.* **75**, 551 (2014).

[19] V. Rajendar. CH. Shilpa Chakra, B. Rajitha, K. Venkateswara Rao, Si-Hyun Park, *J Mater Sci: Mater Electron.* **28**, 3394 (2017).

[20] S. Moradi, P. A. Azar, S.R. Farshid and et al. *Journal of Saudi Chemical Society.* <http://dx.doi.org/10.1016/j.jscs.2012.08.002> (2017).

[21] C.A. Aggelopoulos, M. Dimitropoulos, A. Govatsi, L. Sygellou, et al. *Applied Catalysis B, Environmental.* <http://dx.doi.org/10.1016/j.apcatb.2016.12.023> (2017).

[22] S. Teixeira P.M. Martins S.L. M´endez, K. K`uhn, G. Cuniberti. *Applied Surface Science.* <http://dx.doi.org/10.1016/j.apsusc.2016.05.073> (2017).

[23] R. Ullah, J. Dutta, *Journal of Hazardous Materials.* **156**, 194 (2008).